Zeolitic tuffs for acid mine drainage (AMD) treatment in Ecuador: breakthrough curves for Mn^{2+}, Cd^{2+}, Cr^{3+}, Zn^{2+}, and Al^{3+}

Xavier Buenaño[1] · Laureano Canoira[1] · Domingo Martin Sánchez[2] · Jorge Costafreda[2]

Abstract Zeolitic tuff constitutes a technical and economical feasible alternative to manage acidic waters in initial phases of generation. A study of cation exchange with two zeolitic tuffs from Ecuador and one from Cuba has been conducted using breakthrough curve methodology. Cations Mn^{2+}, Cd^{2+}, Cr^{3+}, Zn^{2+}, and Al^{3+} have been chosen owing to their presence in underground water in exploration activities (decline development) in Fruta del Norte (Ecuador). Zeolites characterized by X-ray diffraction and thermal stability after heating overnight as heulandites show a similar exchange behavior for the five cations studied. The clinoptilolite sample Tasajeras shows a relevant cation exchange performance expressed in the important increment of spatial time to reach the breakthrough point in comparison with heulandite samples. The maximum length of unused beds was found for Cr^{3+} and Zn^{2+} cations showing, therefore, a lower adsorption performance in relation with Mn^{2+} and Cd^{2+}. A final disposal method of metal-loaded zeolites with cement is proposed.

Introduction

Mineral resources such as coal and metal ores such as gold, silver, and copper are often rich in sulfide minerals, reflecting rock or sediment environments generally high in sulfur content and low or devoid of free molecular oxygen (Jacobs et al. 2014). A number of classification schemes of mine waters have been proposed using one or several water parameters, such as major cations and anions, pH, alkalinity vs. acidity, and so forth (Lottermoser 2010). Oxidation of sulfide minerals generates acid mine drainage (AMD), and tropical environments can accelerate this process; therefore, AMD constitutes one of the most important issues in environmental management in mining sector. On the other hand, the precautionary principle is the basis to manage the environmental aspects in any human activity; however, it is not always possible. For this reason, it is critical to find feasible AMD treatments in terms of technical and economic aspects.

The first large-scale mining operations in Ecuador are scheduled for the next years. Fruta del Norte (area located in the southeast of Ecuador) deposit is an intermediate sulfidation epithermal gold-silver deposit measuring 1670 m along strike, 700 m down dip, and generally ranging between 150 and 300 m wide (RPA Inc. 2014). An initial dataset of the AMD water quality, which was obtained in baseline studies from exploratory works in Fruta del Norte (Cardno 2016), has been reviewed to carry out AMD treatment studies for cations that could be out of compliance when mining operations start. Also, the data allow gathering background surface and underground water metal concentration studies.

The treatment process for the removal of the heavy metal cations from AMD includes coagulation, carbon adsorption, ion exchange, precipitation, and reverse osmosis (Eckenfelder 1999). The ion exchange processes are probably the most attractive among these methods, since their application is simple, and they require relatively mild operating conditions, although the cost of ion exchange materials and regeneration is

the limiting factor (Kesraoui-Ouki et al. 1994). There is a huge variety of filter materials for metal removal of AMD; a complete review (Westholm et al. 2014) is provided. Organic (ion exchange resins) and inorganic filter materials have been investigated. Among the inorganic ion exchange adsorbents, natural and synthetic zeolites have the best properties (Iakovleva and Sillanpää 2013) and the cost per metric ton is low. Optimizing its use aims to reduce costs in AMD treatment. It is important to look for low-cost ion exchange materials as natural zeolites that could replace or complement synthetic ion exchange resins. Natural zeolites are the most important inorganic cation exchangers that exhibit high ion exchange capacity, selectivity, and compatibility with the natural environment (Ouki and Kavannagh 1999).

Zeolites are considered an uncommon group of tectosilicates (Ryan 2014). Some types of zeolites have outstanding adsorption properties related with their framework structure and porous size. Cations with similar charges such as K^+, Na^+, Ca^{2+}, and Mg^{2+} can be exchanged in the channels of zeolites. For this reason, these are used in industrial and municipal water treatments; additionally, their non-toxicity characteristic attracts the research interest. The use of natural zeolitic tuffs is restricted to their availability in the surrounding areas of mining operations. In the case of Ecuador, zeolitic tuffs have been identified in the Coast (Machiels 2010).

Natural zeolites are used abundantly as a type of natural pozzolanic material (Ahmadi and Shekarchi 2010). In this context, application of saturated zeolitic tuffs for immobilization of heavy metal cations analyzed in this study from aqueous solutions and later use to prepare building composites is a feasible option. This hypothesis is meaningful if zeolites pass the pozzolanicity test.

The aim of this paper is to assess the use of zeolitic tuffs from Ecuador and Cuba (as a reference material) to treat the potential AMD of the new metallic mining operations mainly located in southeast Ecuador. For this reason, it is necessary to know the material characterization, mineralogy, and water characterization of the study area.

Experimental

Materials

Zeolite-rich tuff samples from Guayas (Ecuador) and Tasajeras (Cuba) as reference material were used to carry out the experimental analysis.

In the case of Ecuador, there are some potential areas of zeolitic tuffs due to the geological configuration of the country with volcanic arc environments at subduction zones, where an important quantity of glass-rich material is erupted and deposited in continental or marine basins. Detailed research has been developed in the Late Cretaceous Coastal Cayo Arch that includes Chongón-Colonche mountain range and surrounding areas (Machiels et al. 2008). One of the most complete sections of the Late Cretaceous stratigraphy occurs in the Guaraguao River, a river located 35 km NW of Guayaquil (Machiels et al. 2014).

Zeolite tuff samples (named as XB_01 and XB_02) studied in this work were taken in the Late Cretaceous Coastal Cayo Arch Ecuador, specifically in the Guaraguao River, showing the most important characteristics of heulandite zeolitic tuffs according to an analysis of preliminary studies (Garcés 2013). The selection of sample location is shown in Fig. 1a.

In the central area of Cuba, zeolitized rocks appear in a 0.7–5-km-wide × 20-km-long area, in southeastern sector of Santa Clara town (Fig. 1b), where Piojillo and Tasajeras deposits are located. Tasajeras deposit is the most important in the region and one of the biggest of this country and belongs to Hilario geological formation (Orozco and Rizo 1998), which is constituted by zeolitized and altered tuffs with varieties from vitroclastic to cristalitoclastic.

For the final experimental phase related with metal-loaded disposition, normalized cement and sand were employed.

Characterization of the zeolites

The determination of mineralogical composition of the zeolitic tuffs XB_01 and XB_02 was carried out with a powder X-ray diffraction (XRD) analysis in a diffractometer Philips PW-1820 with Cu anode ($K_{\alpha 1}$ = 1.54 A) scanning from $2\theta = 4°$ to 60°. The identification of minerals was performed with Diffrac+ Eva software from Bruker, and the diffractograms were compared with those of reference samples (Bayliss et al. 1986). The visualization of diffractograms was carried out with PowderX (Dong 1999).

The patterns belong to clinoptilolite and heulandite zeolitic tuffs as the main component. The secondary components are as follows: feldspar, quartz, albite, illite, and montmorillonite clays. Nevertheless, it is not possible to carry out a differentiation between these two zeolitic tuff types based solely on the XRD results because they share the same peaks. To distinguish between clinoptilolite and heulandite in the zeolitic tuffs, it is necessary to heat the samples at 450 °C overnight and register the XRD pattern afterwards (Calvo et al. 2009). The XRD analyses after heating were carried out in an Empyrean PANalytical X-ray diffractometer. Figure 2 shows the XRD patterns of the three samples as received and after the thermal overnight treatment.

Additionally, an XRD study with thermal treatment in situ (reaction chamber) was carried out in a Bruker D8 A25 X-ray diffractometer provided with Cu and Ag anodes and reaction camera to measure between 0 and 900 °C in air atmosphere. This analysis was carried out with sample XB_01, and it is shown in Fig. 3.

X-ray fluorescence (XRF) spectroscopy analysis was carried out in order to obtain the major element concentrations and, then, the Si/Al ratio of zeolitic tuff samples. XRF data were

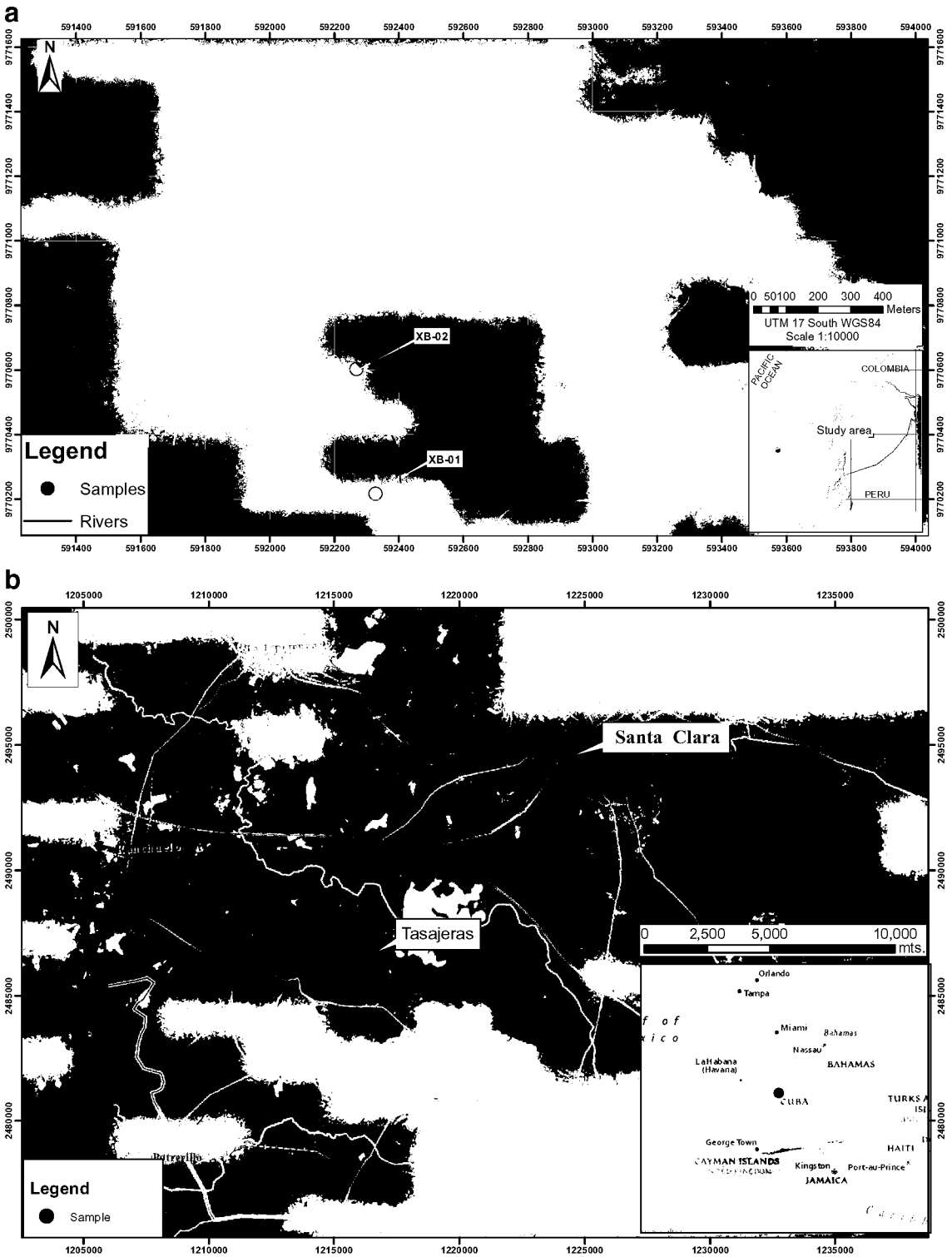

Fig. 1 Sample location map

obtained with a Bruker S8 Tiger A15X10-A3E1A1-C2A1. The chemical composition of zeolites XB_01, XB_02, and Tasajeras is summarized in Table 1. Inductively coupled plasma atomic emission spectroscopy (ICP-AES) was also carried out in order to confirm Al content and gravimetry to get SiO_2 content.

Moreover, thermogravimetric (TG) analyses were carried out with a Q-500 TA Instruments thermal analyzer at a heating rate of 10 °C min^{-1} in the temperature range 24–1000 °C in a nitrogen flow (10 mL/min). Approximately 43 mg of sample was used in each case, and they are shown in Fig. 4.

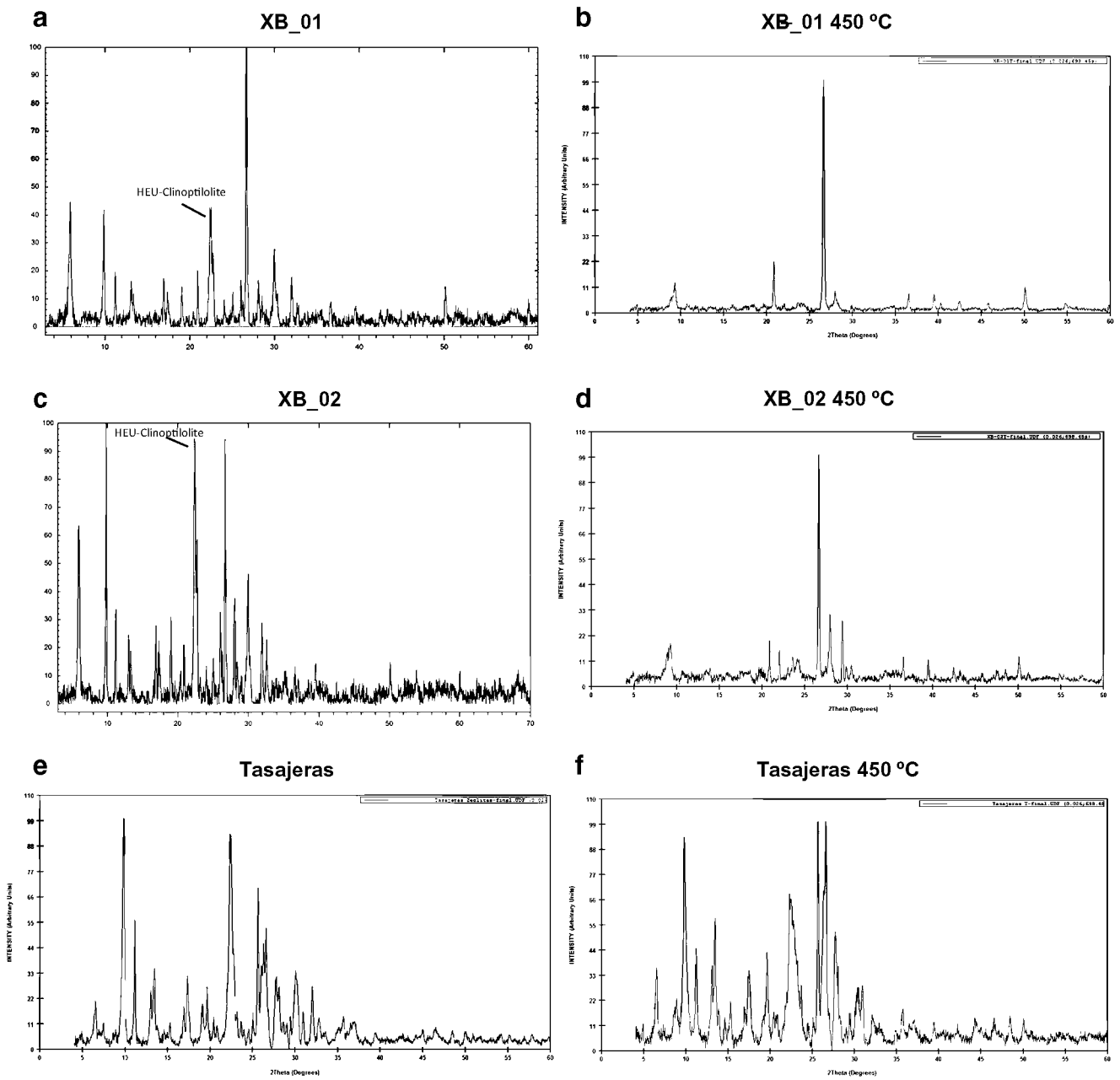

Fig. 2 **a** XRD pattern of XB_01 zeolitic tuff original sample, **b** XRD pattern of XB_01 zeolitic tuff heated overnight, **c** XRD pattern of XB_02 zeolitic tuff original sample, **d** XRD pattern of XB_02 zeolitic tuff heated overnight, **e** XRD pattern of Tasajeras zeolitic tuff original sample, and **f** XRD pattern of Tasajeras zeolitic tuff heated overnight

The zeolitic tuff surface characteristics were defined by BET surface and pore volume with N_2 adsorption method with a degasification temperature of 190 °C in a Quantachrome Instruments Quadrasorb SI equipment during 12 h. The results of these determinations are summarized in Table 2.

Cation exchange capacity

There are some techniques to determine ion exchange capacity. In this case, the process that has been carried out follows the steps described by Calvo et al. (2009). An atomic absorption spectrophotometer (AAS) Analytik Jena contrAA 700 was employed for determination of exchangeable bases. The amount of NH_4^+ ions that left the zeolite phase was determined by visible spectroscopy in a PerkinElmer Lambda 3 UV/vis spectrophotometer.

Cation exchange capacity (CEC) also was determined using a Cuban standard method (Cuban National Bureau of Standards 2008), exchanging the zeolite with a high concentration of NH_4^+ solution, and later release the NH_4^+ cation taken up by the sample with hydrochloric acid and

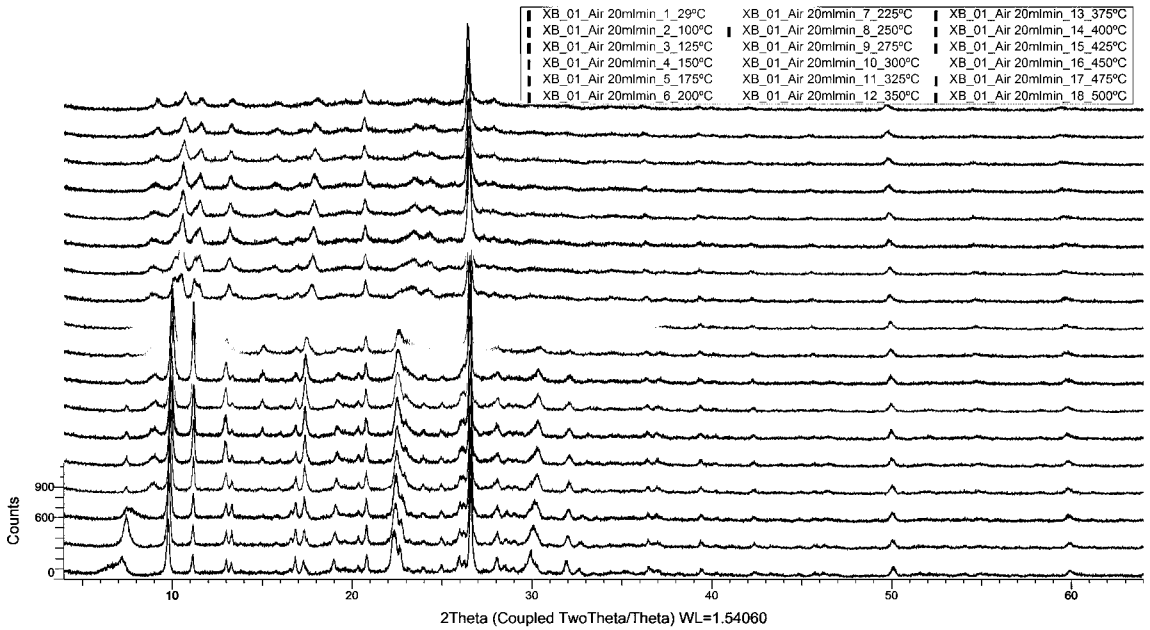

Fig. 3 XRD patterns at different temperatures of XB_01 zeolitic tuff original sample

formaldehyde and titrate the amount of formic acid formed by oxidation of formaldehyde with sodium hydroxide.

The CEC_{bases}, $CEC_{ammonium}$, and $CEC_{Cuban\ standard}$ are summarized in Table 3.

Breakthrough curves

Breakthrough studies were carried out in 15 glass columns (30-cm height × 2-cm inside diameter each) at ambient temperature. Each column was packed with 35 g of zeolitic tuffs (of grain size in the range 1–2 mm) for each cation analyzed; therefore, the experimental bed depth is 10 ± 0.62 cm. The selection of this size was taken in order to optimize the gridding in a practical scenario.

Heights of each column were measured to calculate bed volumes (BV). Flooded conditions were employed to operate the columns, charging the cation loading solutions at the top of the columns. The bottom outlet of columns was fitted with a valve to regulate the flow rate to 262 $cm^3\ h^{-1}$ average (in columns with zeolites XB_01 and XB_02) and to 429 $cm^3\ h^{-1}$ average for zeolite Tasajeras.

Each column was fed with single cation solution salts (Mn^{2+}, Cd^{2+}, Cr^{3+}, Zn^{2+}, and Al^{3+}) according to the concentration analysis of groundwater characterization monitoring program dataset available of exploration decline located in the future mining area. Each solution sample was collected in a labeled plastic bottle of 100 mL and analyzed by AAS.

The hydrated salts used to prepare input solutions were manganese(II) chloride, cadmium(II) chloride 1-hydrate, chromium(III) chloride 6-hydrate, aluminum nitrate 9-hydrate, and zinc(II) nitrate due to its higher water solubility in comparison with other salts. The input cation concentrations were as follows: 19, 18, 11, 18, and 34 mg/L, respectively, and are slightly higher than the monitoring concentrations.

To draw the breakthrough curves, an automatic fitting was the first approach; nevertheless, owing to the important number of measurements carried out and the little range of concentrations analyzed, no good results were found. For this

Table 1 Bulk chemical composition of zeolitic tuffs (wt%) by X-ray fluorescence analysis

Sample	Na_2O	MgO	Al_2O_3	SiO_2	P_2O_5	SO_3	K_2O	CaO	TiO_2	Mn_2O_3	Fe_2O_3	LOI	Si/Al
XB_01[a]	0.557	2.035	10.651	57.668	0.124	0.068	0.427	4.378	0.415	0.064	4.403	14.405	4.570
XB_01	1.996	1.555	10.695	60.123	0.132	0.049	0.813	3.240	0.505	0.137	5.941	10.234	4.770
XB_02	0.951	2.433	12.511	52.504	0.219	0.085	0.649	4.976	0.534	0.113	5.787	15.827	3.570
Tasajeras 1	1.470	0.610	11.760	64.390	–	–	1.290	3.600	0.310	–	1.960	14.570	4.640
Tasajeras 2[b]	1.376	0.947	11.750	66.550	–	–	1.677	2.824	0.278	–	1.430	–	4.820

LOI loss on ignition

[a] Duplicate sample of XB_01

[b] Duplicate sample of Tasajeras

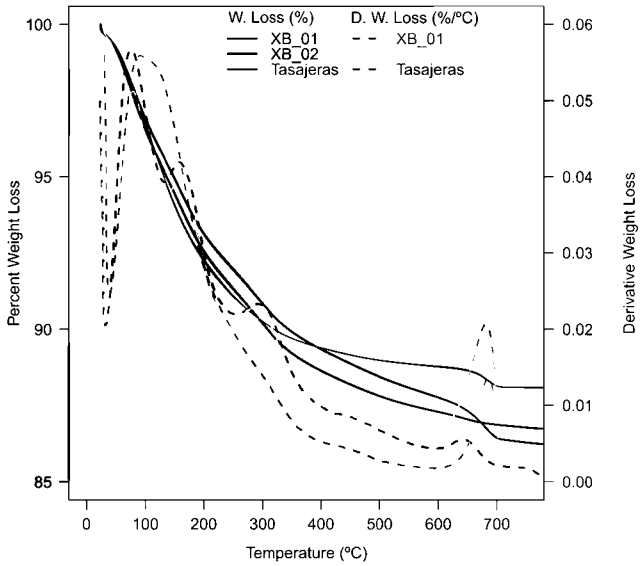

Fig. 4 Thermogravimetric analysis of XB_01, XB_02, and Tasajeras zeolitic tuffs. *Continuous lines* represent percent weight loss, and *dashed lines* represent derivative weight loss for each sample analyzed. *Width lines* identify each sample

reason, the drawing was developed in a manual way, using the R software (R Core 2014). The computation of integration areas was carried out with the same software, and the results were compared with numerical integration, and they are very similar.

Immobilization of metal-loaded zeolites in cements

The pozzolanicity test included storage, filtration, and determination of the hydroxyl ion and calcium oxide concentrations of zeolite samples, according European Standard EN 196-5, 2011. The concentrations are expressed to the nearest 0.1 mmol/L.

The concentrations of calcium ion (expressed as calcium oxide) and hydroxyl ion were plotted as a point. The cement satisfies the test for pozzolanicity when this plotted point is below the curve expressed mathematically by [CaO] = 350 / ([OH] − 15.0) named calcium ion saturation concentration.

A grinding of metal-loaded zeolitic tuffs was carried out in order to get a particle size of 0.063 mm. Samples of 125 g were obtained for XB_01, XB_02, and Tasajeras metal-loaded zeolitic tuffs. A mixture with 375 g of cement, 225 g of water, and 1350 g of standard sand was carried out to obtain three prismatic specimens of 40 mm × 40 mm in cross section and 160 mm in length for each metal-loaded zeolite sample. The laboratory where preparation of specimens took place was maintained at a temperature of 20 ± 2 °C and a relative humidity of not less than 50%.

The specimens were immersed in distilled water in individual containers according each metal-loaded zeolite sample. Also, two containers labeled as P1 and P2 were used as control with specimens of cement mixture of 450 g of cement, 225 g of water, and 1350 g of standard sand. The water of containers was stored in a range of 20 ± 0.5 °C.

The water volume of containers was enough to guarantee that the specimens are always immersed. A weekly water sampling of 50 mL was carried out during a 3-month period. The samples were collected in labeled plastic bottles, and one drop of hydrochloric acid was added to maintain metal species in dissolution. Water samples were analyzed by AAS for cations Mn^{2+}, Cd^{2+}, Cr^{3+}, and Zn^{2+}. Cation Al^{3+} was not considered because it is present in zeolite structure.

Table 2 BET surface and pore volume of the zeolitic tuffs studied

Sample	BET surface ($m^2\ g^{-1}$)	Pore volume ($cm^3\ g^{-1}$)
XB_01	19.40	0.035
XB_02	16.96	0.030
Tasajeras	54.27	0.075

Theory and calculations

The ion exchange reaction is a stoichiometric process. For example, for a binary ion exchange involving a monovalent cation (such as Na^+) and divalent cation M^{2+}, the basic reaction may be written as shown in Eq. 1.

$$2Na_z^+ + M_S^{2+} \Leftrightarrow 2Na_S^+ + LM_z^{2+} \quad (1)$$

where the subscripts z and s refer to the zeolite and solution phases, respectively, and L is defined as a portion of zeolite framework holding unit negative charge. On the other hand, anions are also present in the aqueous solution and maintain electroneutrality in that phase (Güvenir 2005).

In the experiments with zeolitic tuff columns, the test cation concentration in the effluent (C) increments suddenly and approaches the input concentration (C_0), showing ending of ion exchange. Usually, the "breakthrough point" is considered a point where the test cation concentration reaches the 5% of the input concentration ($C = 0.05 \cdot C_0$) (McCabe et al. 1993).

Commonly, the breakthrough point is expressed in terms of breakthrough spatial time, dividing the accumulated volume (mL) of test solution by flow rate (mL min^{-1}). The graphical plot of C/C_0 vs. spatial time is called the breakthrough curve.

The parameters that can be obtained from the breakthrough curve are as follows:

- The breakthrough time, t_b, in hours.
- The weight of test cation exchanged per gram of zeolite until the breakthrough time, W_b (mg cation/g zeolite), according to Eq. 2.

$$W_b = \frac{F_A \int_0^{t_b} \left(1 - \left(C/C_0\right)\right) dt}{d \cdot h} \quad (2)$$

Table 3 CEC for zeolitic tuff samples XB_01, XB_02, and Tasajeras (meq/100 g zeolite)

Sample	Na^+	K^+	Ca^{2+}	Mg^{2+}	CEC_{bases}[a]	CEC NH_4^+	CEC Cuban S.
XB_01	8.74	0.63	88.70	11.13	109.21	74.13	78.62
XB_02	8.09	0.62	106.58	10.39	125.67	55.34	60.40
Tasajeras	71.53	2.87	42.71	2.67	119.78	60.40	124.65

[a] $CEC_{bases} = \Sigma\,[Na^+] + [K^+] + [Ca^{2+}] + [Mg^{2+}]$

CEC Cuban S. Cuban Standard 626

where d is the density (apparent) of zeolite (g cm^{-3}), h is the height of zeolite column (cm), and F_A is the test cation input rate per square centimeter of column section (g cm^{-2} h^{-1}), according to Eq. 3.

$$F_A = \frac{Q \cdot C_0}{1000 \cdot S} \tag{3}$$

where Q is the flow volume of the test cation solution (cm^3 h^{-1}), C_0 is the concentration of the input test cation solution (g cm^{-3}), S is the column section (cm^2), and 1000 is a conversion factor to go from milligrams to grams. The integral shown in Eq. 2 represents the area above the breakthrough curve, and their boundaries are between spatial time = 0 and breakthrough point time (t_b).

The saturation weight (W_{SAT}) is the same expression that of Eq. 2 with the difference that the upper limit of the integral is the saturation time ($C/C_0 = 1$). Thus, the length of unused bed (LUB) is a factor which relates W_b and W_{SAT} according to Eq. 4.

$$\mathrm{LUB} = h\frac{W_b}{W_{SAT}} \tag{4}$$

where h is the zeolite column height (cm).

Figures 5, 6, 7, 8, and 9 show the breakthrough curves for Mn^{2+}, Cd^{2+}, Cr^{3+}, Zn^{2+}, and Al^{3+}, respectively, for zeolitic tuffs tested.

Results and discussion

Characterization of the zeolitic tuffs

The family of zeolites containing the heulandite (HEU) topology with Si/Al ratios ranging between 3 and 5 is the most abundant of the natural zeolites in the environment (Gottardi and Galli 1985). The higher silica member of this family is identified as clinoptilolite, with a Si/Al ratio greater than 4. Heulandites are defined as those minerals with Si/Al ratio below 4. In our samples, the presence in the zeolitic tuffs of variable amounts of quartz and feldspar somewhat makes it difficult to apply these classification criteria.

However, XRD tests were developed in order to confirm that the samples belong to the heulandite-type zeolitic tuffs. Additionally, TG analysis, ICP-AES, and XRF of the samples XB_01 and XB_02 were necessary in order to define the Si/Al ratio and the main mineralogical phases.

There are some differences in the Si/Al ratios obtained between XRF, ICP, and gravimetric techniques. The sample XB_01 has higher Si/Al ratio than XB_02 in all cases. The sample XB_01 with a Si/Al ratio of 4.57 would be considered a clinoptilolite, but the sample XB_02 given by XRF would be considered a Si/Al ratio of 3.57 (heulandite) and 4.44 by ICP gravimetry (clinoptilolite). The key difference between natural heulandite and clinoptilolite is their thermal stability (Calvo et al. 2009).

A clinoptilolite zeolitic tuff from Cuba (Tasajeras deposit (Orozco and Rizo 1998) named as Tasajeras was used in order to confirm the validity of the heating overnight method to distinguish between heulandite and clinoptilolite zeolites. XRD analysis of samples was carried out before and after heating overnight. Figure 2 shows the XRD pattern of XB_01, XB_02, and Tasajeras zeolitic tuffs before and after the heating procedure. The peak d = 8.98 Å (typical in XRD pattern of clinoptilolite) in samples XB_01 and XB_02 disappears in the XRD pattern after the heating overnight (450 °C for 12 h.). Moreover, this peak remains in Tasajeras sample after the heating, showing clearly its clinoptilolite nature.

Figure 3 shows the XRD of reaction chamber results with 18 diffraction patterns at different temperatures for sample XB_01, from 29 to 500 °C with an interval of 25 °C (from 100 °C). The loss of zeolite structure starts to produce in the range of 250 to 275 °C, and the peak of $2\theta = 8.98°$ disappears.

Clinoptilolite belongs to the zeolite group that does not show major structural changes during thermal dehydration processes, which exhibit continuous mass loss curves as a function of temperature. Thus, TG analysis is often used to investigate chemical processes in which weight changes occur.

The TG curves for some clinoptilolite zeolite samples in the Alver et al. (2010) experiment do not show changes in the trend of weight loss; the same pattern is shown for the Tasajeras sample. On the other hand, for XB_01 and XB_02 TG curves, important breaks (at least three) in the range of 0–400 °C are present as shown in Fig. 4. These breaks are easily identifiable in the derivative weight loss curves. In the range of 600–700 °C, a break is common for XB_01, XB_02, and Tasajeras samples. Nevertheless, these changes are not easily recognizable in TG weight loss curves.

The BET surface and pore volume of the zeolitic tuffs studied are summarized in Table 2. Both samples of heulandites from Ecuador XB_01 and XB_02 show very similar results, with low surface areas and very low pore volumes, which could predict a bad exchange behavior in the breakthrough studies, in great contrast with other zeolitic tuffs from Chongón-Colonche coastal arc (Calvo et al. 2009). On the other hand, the clinoptilolite Tasajeras sample shows good BET surface area and pore volume, around three and 20 times, respectively, the values of the Ecuador samples, thus predicting a better exchange behavior.

The CEC has been evaluated by three independent methods: (i) total amount of alkaline and alkaline-earth exchangeable cations (CEC basis), (ii) amount of ammonium cation released by the zeolitic tuffs by exchange with potassium chloride and measured by UV/vis spectroscopy (Nessler method), and (iii) amount of ammonium cation released by the zeolitic tuffs by exchange with hydrochloric acid and formaldehyde and measured by a titration method after the Cuban standard 626. These results are summarized in Table 3. The methods (ii) and (iii) gave practically identical results for the Ecuador zeolitic tuffs considering the experimental error. However, the Tasajeras sample gave very different results with both of these methods. The CEC basis gave always higher results for the three zeolitic tuffs, but this value is practically identical to the method of the Cuban standard for the Tasajeras sample. Thus, taking as the real value for CEC the mean of two coincident values, we could ascertain a CEC of 76.4 meq/100 g zeolite for the sample XB_01, 57.9 meq/100 g zeolite for the XB_02 sample, and 122.2 meq/100 g for the Tasajeras sample, and the prediction is again that with these CEC values, Tasajeras would behave much better in the exchange experiments.

Breakthrough studies

The breakthrough curves constitute a tool to define the sequence of cation affinity of zeolitic tuffs tested in relation with cations studied. A preliminary study (Margeta et al. 2015) has shown that the grain size of the zeolite tuff was not proved to have a significant effect on adsorption in any form of zeolitic tuff (pretreated or natural tuff).

In general terms, the input water concentrations considered in this study are low, but as it was commented before, they are out of limits of legal national compliance, specifically according to discharge limits to a water body (Ministry of Environment of Ecuador 2015) for Mn^{2+}, Cd^{2+}, Zn^{2+}, and Al^{3+}. Examples of more stringent standards which might be imposed depending on circumstances include the following: Zn <0.5 mg L^{-1}, Cr <0.2 mg L^{-1}, Al <0.1 mg L^{-1}, and Cd <0.5 μg L^{-1} (Younger et al. 2002).

In this study, a high quantity of samples was taken in order to draw the curves and to reach the ratio $C/C_0 = 1$. Figures 5, 6, 7, 8, and 9 show the breakthrough curves for Mn^{2+}, Cd^{2+}, Cr^{3+}, Zn^{2+}, and Al^{3+}. In all breakthrough curves, breaks appear linked with experiment interruptions in weekends as it happens in other studies (Calvo et al. 2009). The abundance of experimental points allows to identify these breaks easily and traces the curve along a general trend. In the case of Cr^{3+} cation, the input concentration was the lowest, and therefore, the analysis range was narrower and it was more challenging to trace the curve.

The behavior in terms of adsorption between zeolites XB_01 and XB_02 is very similar for all the cations analyzed. Tasajeras zeolite used as control has shown better adsorption capacity due to its clinoptilolite nature. The breakthrough curves for Al^{3+} do not show any retention time in the three zeolitic tuffs tested. The aluminum is part of the framework structural composition of zeolites, and its interchange is not a favorable process.

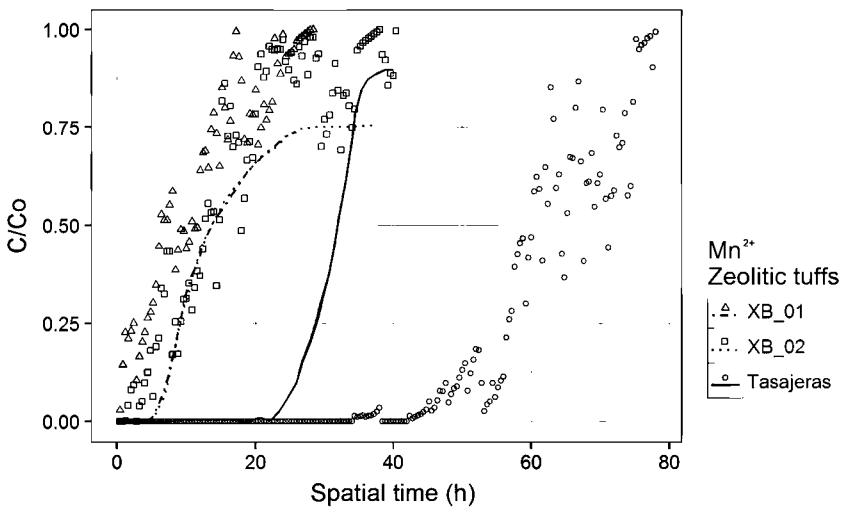

Fig. 5 Breakthrough curves for Mn^{2+}

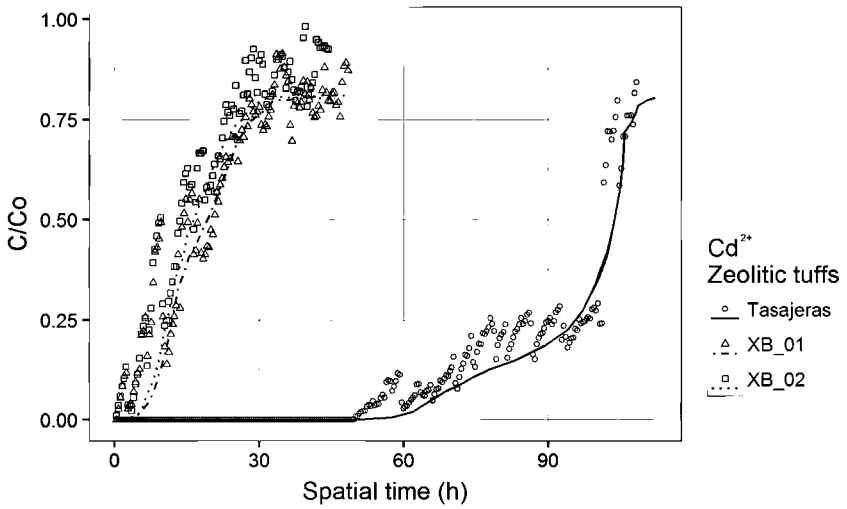

Fig. 6 Breakthrough curves for Cd^{2+}

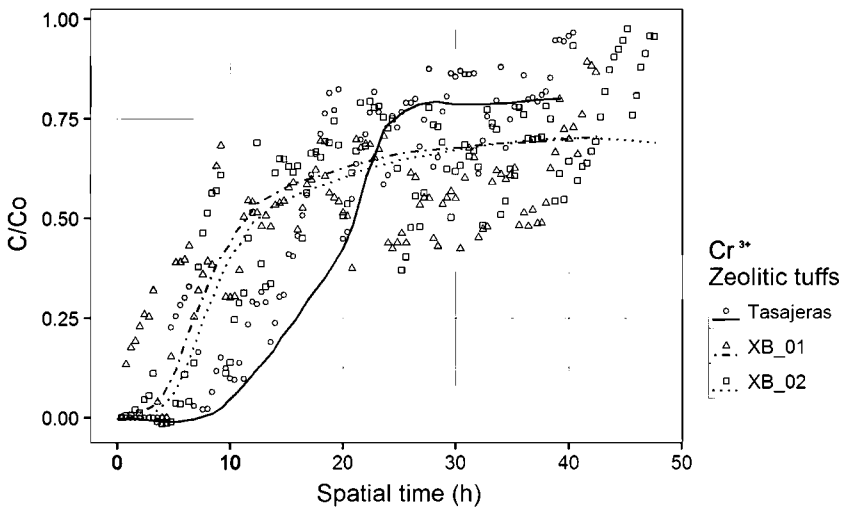

Fig. 7 Breakthrough curves for Cr^{3+}

The breakthrough curve parameters described in the "Theory and calculations" section are summarized in Table 4 for all cations studied. For the Mn^{2+} cation, XB_01 and XB_02 show identically bad parameters, but Tasajeras shows a much better performance, with a t_{SAT} ratio of 1.56 and a t_b ratio of 3.71. The same fact would be observed for the W_{SAT}

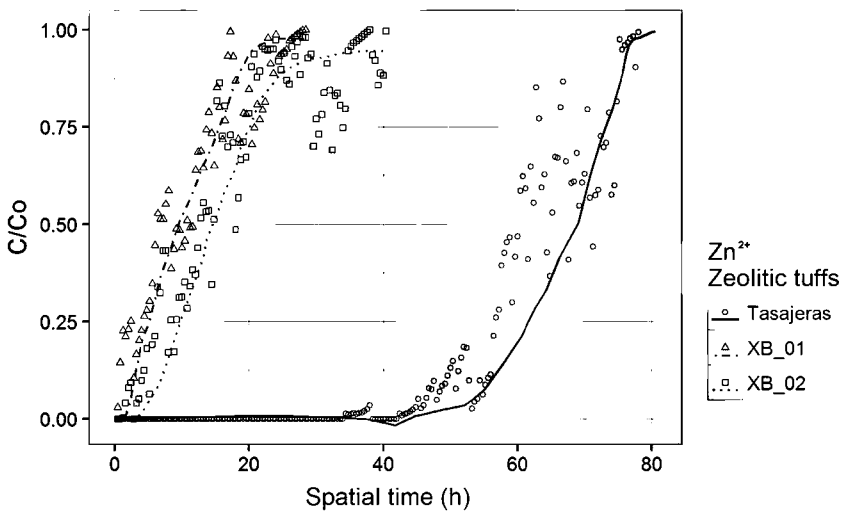

Fig. 8 Breakthrough curves for Zn^{2+}

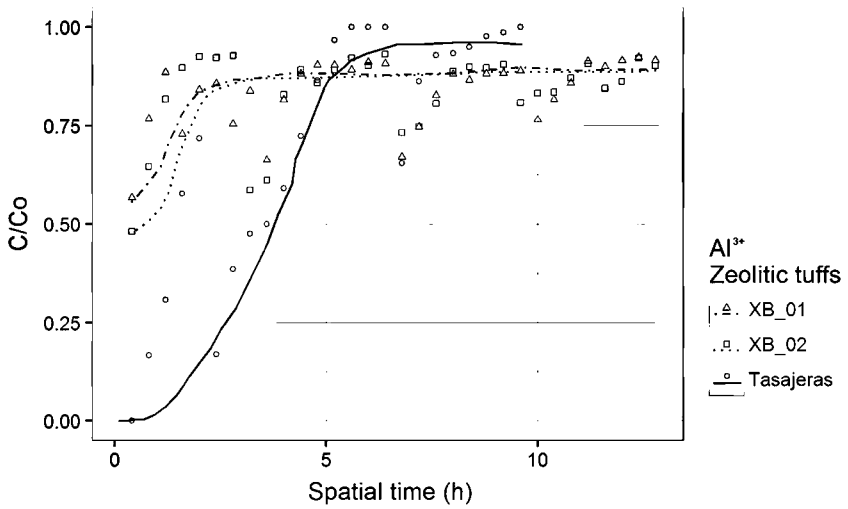

Fig. 9 Breakthrough curves for Al^{3+}

ratio, of more than 3.5 and the W_b ratio larger than 5.5. Finally, the length of unused bed (LUB) for Tasajeras is almost half of those for XB_01 and XB_02.

In relation with Cd^{2+} cation, XB_01 and XB_02 show similar parameters, with the exception of W_{SAT} parameter that shows a little difference. The Tasajeras sample shows better parameters than heulandite samples, and in relation with Mn^{2+}, these improve almost twice; nevertheless, in general, LUB increases a little in comparison with Mn^{2+}.

For the Cr^{3+} cation, it is difficult to get conclusions in relation with adsorption parameters calculated between zeolitic tuff samples because the input concentration of Cr^{3+} cation was the lowest of the cations analyzed in this study. For this reason, the drawing of the breakthrough curve was complicated and the final graph has an important level of uncertainty.

In relation with Zn^{2+} cation, XB_01 and XB_02 show similar parameters, with the exception of W_{SAT} and t_b parameters, where the XB_02 sample has better performance that is reflected in a lower LUB. The Tasajeras sample has a LUB parameter (average) of 4.5 times those of XB_01 and XB_02. In general, it has the best adsorption parameters of the cations analyzed and has the lowest LUB of all the experiments.

Finally, for Al^{3+} cation, XB_01, XB_02, and Tasajeras adsorption parameters show almost the same values. A slight difference in the parameters W_{SAT} and t_b between Ecuador heulandites and Tasajeras can be appreciated; nevertheless, the LUB is almost equal. The worst adsorption results were found with this cation.

On the other hand, the size of the ion that will be treated with a specific zeolite is a critical point (Calvo et al. 2009); for

Table 4 Experimental parameters employed in breakthrough studies for cations Mn^{2+}, Cd^{2+}, Cr^{2+}, Zn^{2+}, and Al^{3+}

Cation	Zeolitic tuff	F_A (mg cm^{-2} h^{-1})	t_{SAT} (h)	W_{SAT} (μg g^{-1})	t_b (h)	W_b (μg g^{-1})	LUB (cm)
Mn^{2+}	XB_01	1.342	25.000	1.697	7.000	0.885	4.690
	XB_02	1.244	25.000	1.593	7.000	0.828	4.540
	Tasajeras	2.117	39.000	6.023	26.000	4.913	2.010
Cd^{2+}	XB_01	1.278	32.000	2.629	8.000	1.046	5.430
	XB_02	1.184	32.000	2.008	8.000	0.854	5.660
	Tasajeras	2.016	110.000	19.197	65.000	12.059	3.770
Cr^{3+}	XB_01	0.760	42.000	1.504	4.000	0.297	7.540
	XB_02	0.704	42.000	1.433	6.000	0.405	6.650
	Tasajeras	1.199	32.000	2.595	8.000	0.961	6.160
Zn^{2+}	XB_01	1.260	25.000	1.227	2.500	0.289	7.670
	XB_02	1.167	25.000	1.631	6.000	0.642	5.920
	Tasajeras	1.987	78.000	11.667	57.000	9.854	1.740
Al^{3+}	XB_01	2.447	12.500	0.533	1.000	0.170	6.400
	XB_02	2.276	12.500	0.466	1.000	0.145	7.300
	Tasajeras	3.860	8.000	1.325	1.400	0.489	6.730

Table 5 Radii and hydration energies for cations tested

Cation	Hydrated radius (Å)	Unhydrated radius (Å)	Free energy of hydration (kJ/mol-ion)
Mn^{2+}	4.38	0.83	−1745.1
Cd^{2+}	4.26	0.97	−1802.4
Cr^{3+}	4.61	0.80	−1797.4
Zn^{2+}	4.30	0.74	−1917.9
Al^{3+}	4.80	0.53	−531.4

this reason, it is important to review this variable. In Table 5 (Carvalho et al. 2005), hydrated, unhydrated radius, and free energy of hydration are shown. However, the hydrated radius of all cations tested is very similar, and thus, no appreciable differences were found for the Mn^{2+}, Cd^{2+}, Cr^{3+}, and Zn^{2+} cations and only Al^{3+} shows a somewhat different behavior that could be due to its greater hydration radius (which could hinder its adsorption by any zeolite) or more probably due to the fact that Al^{3+} is part of the framework structure of all zeolites.

A preliminary study (Iakovleva and Sillanpää 2013) has found that the presence of competing ions did not affect iron adsorption. For this reason, in the current study, an individual cation analysis has been carried out.

Column studies have shown that natural zeolites are capable of removing heavy metals from a continuously flowing solution, and thus, breakthrough curves determine the operating life span of the fixed adsorbent bed (Motsi 2010), and this study confirms this assumption.

Immobilization of metal-loaded zeolites in cements

The zeolitic tuffs XB_01, XB_02, and Tasajeras fulfill the test for pozzolanicity because the points plotted are below the curve of calcium ion (expressed as calcium oxide) saturation concentration according to European standard as shown in Fig. 10.

The analysis results of water samples taken during the study of immobilization of metal-loaded zeolites in cements are summarized in Fig. 11. The analysis confirms that the three samples XB_01, XB_02, and Tasajeras did not leach cations Mn^{2+}, Cd^{2+}, Cr^{3+}, and Zn^{2+} to the water. For graphical purpose, the noise of analytical method has been included (negative concentrations). Neither the control water samples presented any cation concentration.

The room conditions did not show any important change according to the records analyzed. The water pH was recorded at 12.4 ± 0.1 namely basic conditions. These conditions are linked with the pozzolanic materials that react with water at normal ambient temperature dissolving calcium hydroxide to create strength, developing calcium silicate and calcium aluminate compounds.

Conclusions

The mineralogical characterization of materials for acid mine water treatment constitutes a critical phase to approach a good mining. In the case of zeolitic tuffs due to its significant spatial variability, this characterization is particularly critical. XRD with reaction chamber technique constitutes a better alternative to distinguish between clinoptilolite and heulandite zeolites instead of application of XRD before and after heating overnight methodology.

The use of zeolitic tuffs for AMD treatment shows that the heulandite zeolites from Ecuador have, in general, an acceptable performance at low concentrations (less than 20 mg/L) for Mn^{2+}, Cd^{2+}, Cr^{3+}, and Zn^{2+}.

The clinoptilolite from Tasajeras shows the best exchange behavior for these cations, because the spatial times W_b and W_{SAT} increase in orders of three to eight times in relation with heulandites XB_01 and XB_02 from Ecuador.

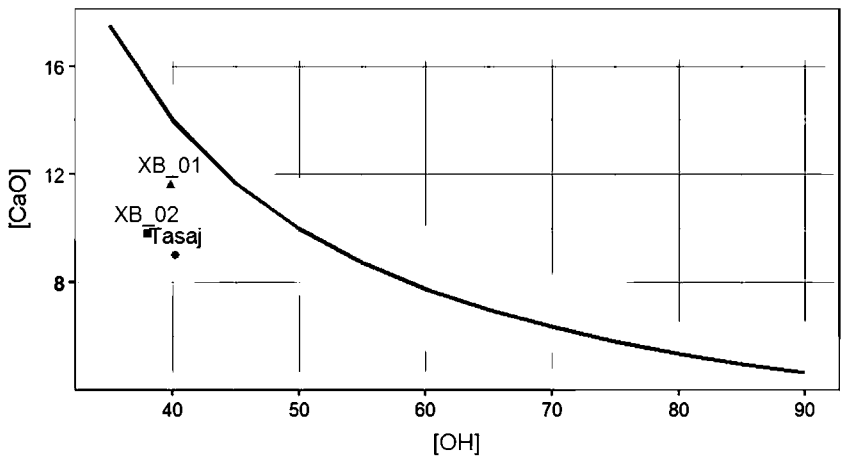

Fig. 10 Pozzolanicity curve test for XB_01, XB_02, and Tasajeras zeolitic tuffs

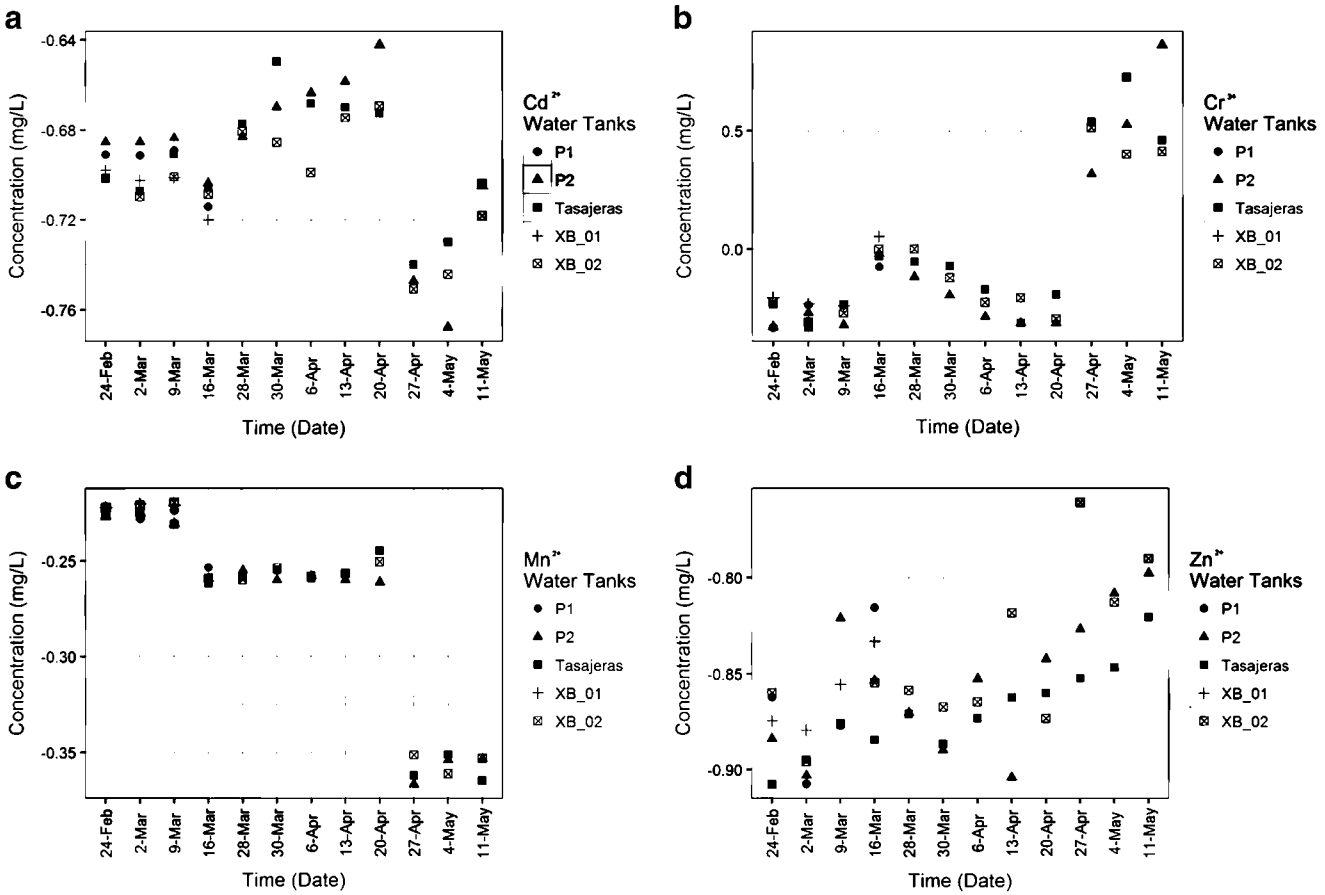

Fig. 11 Analysis of water exposed to metal-loaded zeolites in cements: **a** cation Cd^{2+}, **b** cation Cr^{3+}, **c** cation Mn^{2+}, and **d** cation Zn^{2+}

In the case of Al^{3+} cation, due to the fact that this cation constitutes part of the zeolite framework, no good results were found in any of the zeolites analyzed.

The immobilization of metal-loaded zeolites in cements shows to be a feasible alternative to this type of waste, at least at the cation concentrations tested and considering that XB_01, XB_02, and Tasajeras zeolitic tuffs pass the pozzolanicity test. Other lixiviation tests could be carried out in order to confirm the immobilization of pollutants in zeolites.

Acknowledgments Xavier Buenaño wishes to thank SENESCYT Ecuador for a research grant (262-2012). The authors wish to acknowledge to MSc Emilio García from Universidad Politécnica de Madrid and Prof. José Rodríguez Fernández from Universidad de Castilla La Mancha for the TG analyses; MSc Salomón Brito, MSc Flavio López, and Eng. Angel Valdiviezo from Instituto de Investigación Geológico Minero Metalúrgico de Ecuador (INIGEMM) for the field sampling support and XRF measurements; Dra. Jenny Estupiñán, Eng. Galo Montenegro, and Eng. Washington Vilema from Centro de Investigaciones Geológicas de Petroamazonas EP for XRD support; Dr. David Serrano from IMDEA Energía for XRD with chamber camera analysis; and Eng. Guillermina Blázquez and Eng. Esteban Estévez from Laboratorio Oficial para Ensayo de Materiales de Construcción (LOEMCO) for laboratory support in immobilization of metal-loaded zeolites in cement survey.

References

Ahmadi B, Shekarchi M (2010) Use of natural zeolite as a supplementary cementitious material. Cem Concr Compos 32(2):134–141

Alver BE, Sakizci M, Yörükoğullari E (2010) Investigation of clinoptilolite rich natural zeolites from Turkey: a combined XRF, TG/DTG, DTA and DSC study. J Therm Anal Calorim 100(1):19–26

Bayliss P, Erd D, Mrose M, Sabina A, Smith D (1986) Mineral powder diffraction file. JCPDS, USA 271

Calvo B, Canoira L, Morante F, Martínez-Bedia JM, Vinagre C, García-González E, Alcantara R (2009) Continuous elimination of Pb^{+2}, Cu^{+2}, Zn^{+2}, H^+ and NH_4^+ from acidic waters by ionic exchange on natural zeolites. J Hazard Mater 166(2):619–627

Cardno (2016) Actualizacion del Estudio de Impacto Ambiental del proyecto minero Fruta del Norte, para la fase de Explotacion e Inclusion de las Fases de Beneficio, Fundicion y Refinacion de minerales metalicos. Technical Paper (in Spanish). 10480914. http://www.lundingold.com/i/pdf/eia-2016-esp/EIA_FDN.pdf. Aurelian Ecuador S.A

Carvalho WA, Mandelli D, Dal Bosco SM, Jimenez RS, Figueiredo FCA (2005) Uses of Brazilian natural zeolite in the removal of toxic metal cations from wastewater. Stud Surf Sci Catal 158(Part B):2105–2112

Cuban National Bureau of Standards (2008) *Cuban standard 626, natural zeolites—determination of total interchange cation capacity—ammonium chloride method* (in Spanish)

Dong C (1999) PowderX: Windows-95-based program for powder X-ray diffraction data processing. J Appl Crystallogr 32(4):838–838

Eckenfelder WW (1999) Industrial water pollution control (3rd ed.). McGraw-Hill, Richmond

European Committee for Normalization EN 196-5 (2011) *International norm: cement-test methods—pozzolanicity test for pozzolanic cement*

Garcés D (2013) Mineralogical characterization of natural zeolites deposit in Guaraguao river (Isidro Ayora, Guayas province) and application in ammonium removal in wastewaters. *Escuela Superior Politécnica Del Litoral* (in Spanish)

Gottardi G & Galli E (1985) In Springer (Ed.), *Natural zeolites, 409 p.* Berlin: Springer

Güvenir Ö (2005) *Synthesis and characterization of clinoptilolite (Master's thesis)* doi:http://citeseerx.ist.psu.edu/viewdoc/download?doi=10.1.1.632.6036&rep=rep1&type=pdf

Iakovleva E, Sillanpää M (2013) The use of low-cost adsorbents for wastewater purification in mining industries. Environ Sci Pollut Res 20(11):7878–7899

Jacobs J, Lehr J, Testa S (2014) Acid mine drainage, rock drainage, and acid sulfate soils: causes, assessment, prediction, prevention, and remediation. Wiley, New York

Kesraoui-Ouki S, Cheeseman CR, Perry R (1994) Natural zeolite utilisation in pollution control: a review of applications to metals' effluents. J Chem Technol Biotechnol 59(2):121–126

Lottermoser B (2010) Mine wastes: characterization, treatment and environmental impacts. Springer Science & Business Media, Heidelberg

Machiels L, Garcés D, Snellings R, Vilema W, Morante F, Paredes C, Elsen J (2014) Zeolite occurrence and genesis in the Late-Cretaceous Cayo arc of coastal Ecuador: evidence for zeolite formation in cooling marine pyroclastic flow deposits. Appl Clay Sci 87: 108–119

Machiels L, Morante F, Snellings R, Calvo B, Canoira L, Paredes C, Elsen J (2008) Zeolite mineralogy of the Cayo formation in Guayaquil, Ecuador. Appl Clay Sci 42(1):180–188

Machiels L (2010) *La roca mágica-zeolite occurrence and genesis in the late cretaceous Cayo arc of coastal Ecuador* (PhD Thesis). doi: https://lirias.kuleuven.be/handle/123456789/284432

Margeta K, Stefanović ŠC, Kaučič V, Logar NZ (2015) The potential of clinoptilolite-rich tuffs from Croatia and Serbia for the reduction of toxic concentrations of cations and anions in aqueous solutions. Appl Clay Sci 116:111–119

McCabe WL, Smith JC & Harriott P (1993) *Unit operations of chemical engineering* McGraw-Hill New York

Ministry of Environment of Ecuador (2015) *Official register no. 387*

Motsi T (2010) *Remediation of acid mine drainage using natural zeolite* (PhD Thesis). doi:http://etheses.bham.ac.uk/683/1/Motsi10PhD.pdf

Orozco G, Rizo R (1998) Natural zeolites deposit from Cuba. Acta Geológica Hispánica 33(1):335–339

Ouki S, Kavannagh M (1999) Treatment of metals-contaminated wastewaters by use of natural zeolites. Water Sci Technol 39(10):115–122

R Core T (2014) *R: a language and environment for statistical computing. R Foundation for Statistical Computing*

RPA Inc. (2014) *Technical report on the mineral resource estimate, Fruta del Norte project, Ecuador.* doi:http://www.lundingold.com/i/pdf/technicalreports/2014_10_21_Technical_Report.pdf. Accessed 20 April 2016

Ryan P (2014) Environmental and low temperature geochemistry. Wiley, West Sussex

Westholm LJ, Repo E, Sillanpää M (2014) Filter materials for metal removal from mine drainage—a review. Environ Sci Pollut Res 21(15):9109–9128

Younger PL, Banwart S, Hedin RS (2002) Mine water: hydrology, pollution, remediation. Springer Science & Business Media, Dordrecht